ACS OMEGA

http://pubs.acs.org/journal/acsodf

Article

Investigation of the Temperature Dependence of the Chemical−Mechanical Properties of the Wufeng−Longmaxi Shale

Xu Yu, Cheng Zhai,* Yu Jing, Shuxun Sang, Yu Wang, Klaus Regenauer-Lieb, and Yong Sun

Cite This: *ACS Omega* 2022, 7, 44689−44697

Read Online

ACCESS | Metrics & More | Article Recommendations

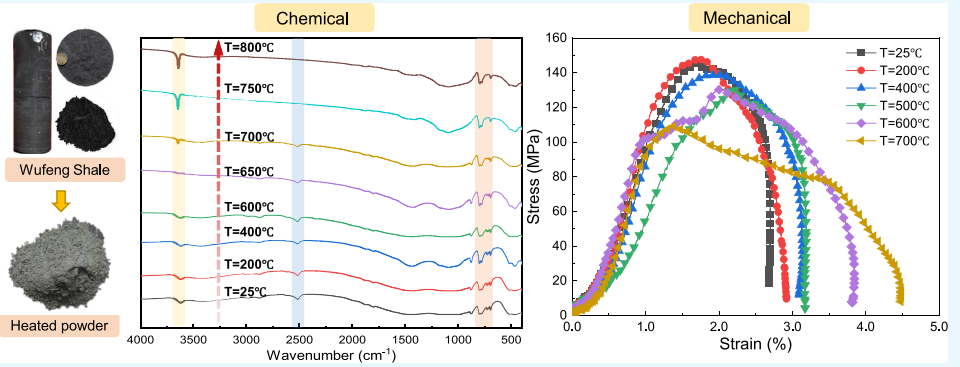

ABSTRACT: Shale rocks have been widely investigated to evaluate the productivity of oil/gas. The high temperature generated by the explosive fracturing to stimulate the gas reservoir has a significant impact on the chemical−mechanical properties of shale rocks. Pioneering works have been carried out at temperatures below 500 °C, but little has been done to quantify the correlation between the chemical and mechanical properties of shale at temperatures above 500 °C. Therefore, an experimental study on the effect of temperature on the chemical−mechanical properties of shale rocks is presented in this paper. The temperatures used in our experiments are between 0 and 800 °C. Results indicate that there exist strong chemical reactions leading to a big reduction in the sample's weight and mechanical strength for a temperature over 500 °C. Thermogravimetric analysis data demonstrates that the weight of shale powders has little change below 400 °C and largely decreases after 600 °C. It shows that the chemical reaction rate corresponding to shale compositions varies with temperature. X-ray diffraction and Fourier transform infrared are integrated to quantify the occurrence of contained reactions including the decomposition of kerogen, carbonates, and quartz transition. This can provide a temperature range for all possible reactions. Changes in the compositional information of shale samples have been proven to significantly influence the mechanical properties. A 25% decrease in dynamic Young's modulus emerges as the temperature approaches 700 °C. As the brittle minerals, for instance, carbonates, decrease with temperature, a brittle-ductile transition happens in shale. This work provides very meaningful results different from that at low temperatures to help people better understand the effects of high temperatures in many fields, such as explosive fracturing and radioactive waste disposal.

1. INTRODUCTION

The rising global demand for hydrocarbon energies has attracted the interest of researchers and engineers in the exploration and development of alternative resources.[1,2] Shale gas, as an unconventional natural resource, can largely ease the worldwide energy crisis. Numerous shale gas development operations have been built, especially in North America, Europe, China, etc.[3,4] However, challenges still exist in recovering shale gas due to the extremely low permeability of the reservoir rock. Explosive methods for enhancing gas production have been applied in the gas/oil industry for decades, for instance, the perforation in the hydraulic fracture and the gas/solid explosives for reservoir fracturing. High temperature generated by the above explosive methods plays a significant role in the properties of the shale gas reservoir.[5] The temperature dependence of the hydro-mechanical properties of gas/shale reservoirs is found. The elevated temperature can also change the chemical composition of shale. It has been identified as a pivotal parameter in shale gas production and has many applications in many fields, such as the evaluation of shale gas productivity[6,7] and gas sorption capacity.[8,9] Up to date, it is difficult to quantify the effects of high temperature on

Received: June 8, 2022
Accepted: November 17, 2022
Published: November 28, 2022

Table 1. List of Clay and Mineral Contents of the Wufeng Shale

	mineral content (%)					clay content (%)		
sample	quartz	calcite	plagioclase	dolomite	total clay	illite	kaolinite	chlorite
Wufeng–Longmaxi shale	33.5	17.3	1.5	36.2	11.5	94	2	4

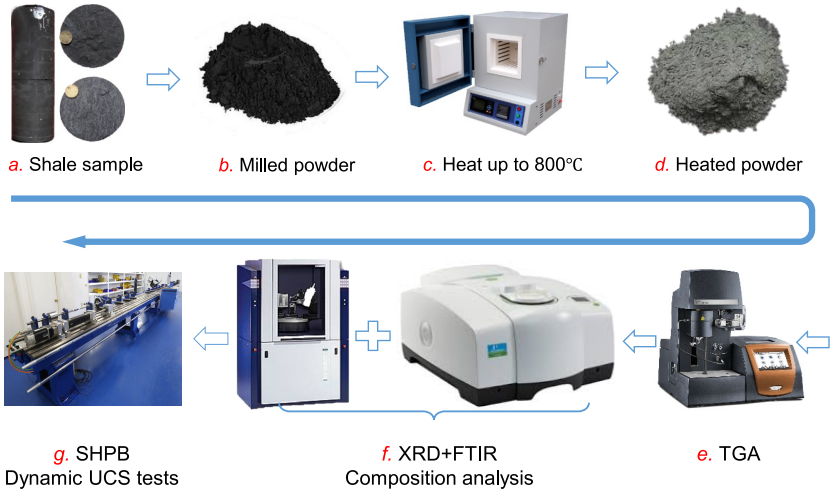

Figure 1. (a–g) Schematic workflow for sample preparation and analysis.

shale formations including the changes in mineral composition and mechanical properties.[10] Therefore, we propose a quantitative method to characterize the effects of temperature on the chemical–mechanical properties of shale rocks.

The temperature-dependent properties of shale have been investigated by many scientists and engineers to evaluate gas production and waste-storage performance. Pioneering works on the effect of temperature on the mechanical behaviors of rocks have been well documented through direct experimental observation and numerical simulations. The work by Masri et al. shows a reduction of Young's modulus and compression failure strength but an increase in the overall deformation of shale samples due to the elevated temperature.[11] Braun et al. found that shale composition affects its pore structure and gas storage potential.[12] Zhou et al. found that the thermal strain rate of shale increases rapidly at 200, 350, and 400 °C directly observed through experimental methods.[13] Similar conclusions had been made on the thermal effects on the mechanical properties of clay, mudstone, and sandstone in many publications.[14−16] Otherwise, mineralogy, particularly the ratio of clay and quartz, frequently appears to be an important factor to assess the mechanical properties of sedimentary rocks.[17,18] For example, the proportion of brittle minerals of quartz and carbonates has been widely used as a brittleness index to assess the feasibility of hydraulic fracturing.[19,20] The chemical compositions and the thermal stability are both fundamental for evaluating the mechanical properties of geomaterials. To date, the hydro-mechanical properties and mineralogy of rocks have been separately investigated in most cases. Little attention has been paid to the correlation of the chemical composition and mechanical properties of shale under different temperatures.

To quantify the minerals of rocks, many experimental facilities have been used including thermogravimetric analysis (TGA), X-ray diffraction (XRD), and Fourier transform infrared (FTIR) spectroscopy.[21−24] TGA is widely used to characterize thermal degradation and temperature-dependent devolatilization of clayey rocks.[22,25] The reported TGA measurements by the previous researchers operated at temperatures up to 400 °C for shale gas/oil production. FTIR spectroscopy is a non-destructive alternative technique to quantitatively assess the mineralogical composition of sedimentary rocks, such as coal and shale. The organic and mineral contents of rock samples can be estimated from FTIR spectra in the mid-infrared spectral region (4000–400 cm^{-1}).[26,27] Previous studies have proven its feasibility in the applications of acquiring quantitative compositional information from geomaterials. XRD and FTIR are primarily used for chemical identification and structural study.[24,28] In recent decades, they have been increasingly applied in the quantitative mineral analysis of sedimentary rocks.

A general method integrating the TGA, XRD, and FTIR techniques has been proposed by Bhargava et al.[21] and Fan et al.[24] to quantify the compositional change in shale rocks at various temperatures. It shows a good agreement with the published data.[21] Now, the combined technique instead of a single technique has been widely used all around the world. It has an advantage in the quantitative characterization of compositional information of shale rocks with a high resolution. Herein, the combined technique integrating TGA, XRD, and FTIR is applied in this work. We conducted a study to characterize the effect of temperature on the chemical–mechanical properties of shale reservoirs. The contents of this paper are listed as follows. Section 2 presents the workflows for sample preparation and methodology. Then, the corresponding results of all experiments and analyses are shown in Section 3. Section 4 demonstrates the discussions. Finally, conclusions are drawn in Section 5.

2. EXPERIMENTAL METHODS

2.1. Sample Preparation. Gas shale samples studied in this work were obtained from the southeast area of Sichuan Province in China, where the shale gas has been successfully produced commercially.[29] They belong to the geologically

https://doi.org/10.1021/acsomega.2c03575
ACS Omega 2022, 7, 44689−44697

defined Wufeng−Longmaxi formation. Early literature on the characteristics of the corresponding shale properties has revealed a long-term and high productivity of the shale gas.[30,31] The shale formation located in the Jiaoshiba area of Sichuan is the reservoir of the first commercial shale gas project in China with an annual production rate of 5×10^8 m^3. Shale rocks have high ratios of quartz and clay minerals.[20,32] The clay and mineral contents of the selected shale sample are listed in Table 1. The weight ratios of quartz and carbonates are 33.5 and 55.0%, respectively, which are slightly higher than the averaged data. The proportion of the clay in the sample is small. The observed carbonate minerals include calcite (17.3%), dolomite (36.2), and plagioclase (1.5%).

Figure 1 demonstrates the workflow of sample preparation and all experimental tests. First, the shale rocks were crushed and milled into 325 mesh (36 μm). Second, 10 g of shale powder was sent for the thermogravimetric analysis (TGA). Then, a muffle furnace was used to heat the shale powder to various temperatures. In this work, we selected eight different temperatures of the room temperature (25 °C), 100, 200, 400, 600, 650, 700, 750, and 800 °C, for heating the shale powder. Each sample was kept in the muffle furnace for an hour at a fixed temperature. Third, XRD and FTIR were combined to measure the compositions of the heated powders.

2.2. TGA. Thermogravimetric analysis (TGA) of the shale samples was undertaken using a USTA 55 thermogravimetric analyzer with a temperature precision of ±0.1. In this work, 1.0 g of shale powder with a particle diameter of less than 36 μm was evenly distributed on a platinum pan and used for TGA tests. The initial TGA temperature for all samples was 25 °C, and the final temperature was 800 °C with a heating rate of 10 °C/min. The tests were carried out under nitrogen purging at a rate of 20 mL/min to eliminate the oxidation of shale powders.

2.3. XRD and FTIR. X-ray diffraction analysis was conducted with a Bruker XRD D8 advance diffractometer equipped with a ceramic tube, X-ray source, a monochromator, an automatic variable divergent slit, and a 1.0 mm detector slit. The step size for the increment of the angle theta was 0.01 °C. It has wide applications including phase identification, quantitative phase analysis, and microdiffraction. Samples for XRD measurements were carefully ground rock powders or fine size fractions separated by centrifugation or gravity settling. Ideally, the concentration of the mineral phases of interest should be more than several percent. If not, it will be difficult to accurately identify the interesting phase.

The shale powders heated at various temperatures were analyzed by a Nicolet iS50 infrared spectrometer. FTIR spectra were collected in the mid-IR range (4000−400 cm^{-1}) for all shale samples with 4 cm^{-1} resolution (2 cm^{-1} steps). Therefore, there are a total of 1801 data points for each spectrum from 4000 to 400 cm^{-1}.

2.4. SHPB Tests. To verify the correlation between temperature and the mechanical properties of shale, we carried out a series of tests with the split Hopkinson pressure bar (SHPB) to directly observe the evolution of the dynamic mechanical properties. The samples collected from Wufeng shale were shaped into Brazilian discs with a size of $\varphi 50 \times 25$ mm and subsequently heated in a muffle furnace to reach 25, 200, 400, 500, 600, and 700 °C. The SHPB loading is perpendicular to the bedding plane of shale. Experimental parameters, peak strength, strain rate, maximum strain, and dynamic compressive strength in the SHPB measurements are listed in Table 3. The measured strain rates in this work were between 60 and 90 s^{-1} at an initial gas pressure of 0.60 MPa.

3. RESULTS

3.1. TG-DTG Analysis. Figure 2 illustrates the results of the TGA analysis for the Wufeng shale powders. The red line is the TG curve representing the evolution of sample weight for temperature ascending. The sample's weight has been found having little reduction before 400 °C, but a significant change emerges at a temperature of 600−750 °C. It may be caused by the decomposition of carbonates. To analyze the weight loss rate, we also come up with the derivative thermogravimetric (DTG) curve calculated from the thermogravimetric (TG) curve. Up to 400 °C, a very small weight loss of 2.66% can be the result of the loss of moisture and the interlay water from clay minerals. It is consistent with the data reported in previous literature.[22,33] However, up to now, the specific temperature for structural water in the clay minerals to release is not clear.

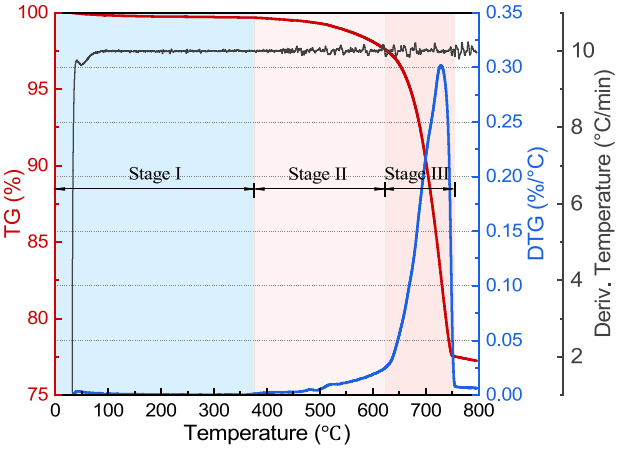

Figure 2. TG-DTG curves of weight evolution of the shale sample.

At the region of 400−600 °C, the weight loss rate slightly increases and some carbonate types contribute to the weight loss in this region. The work by Galan et al. shows that a large fraction of kerogen is decomposed at around 500 °C, but the decomposition amount varies from sample to sample due to the different kerogen concentrations.[14,34] Figures 2 and 3 show that the largest weight loss occurs in the temperature region of 600−750 °C.

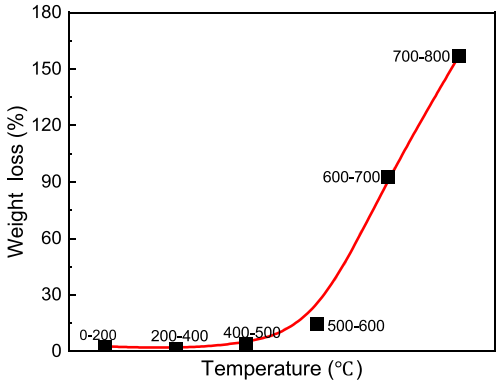

Figure 3. Accumulated mass loss in the different temperature ranges.

https://doi.org/10.1021/acsomega.2c03575
ACS Omega 2022, 7, 44689−44697

The sample's weight reduces with the elevated temperature, which is divided into three stages according to the derived weight loss rate (Table 2). Stage I is when the temperature is less than 400 °C, where the weight change by moisture loss is the minimum. In Stage II, the organic and mineral matter may start to decompose when the temperature is 400−620 °C, causing little weight loss. Stage III is when the temperature is over 600 °C, and a rapid weight reduction occurs as the result of the further decomposition of carbonate minerals, such as calcite, dolomite, and ankerite.

Table 2. Three Stages of Shale Weight Loss with the Evolution of Temperature

stages	temperature (°C)	decomposed matters of shale rocks
I	<400	moisture and interlayer water of clay minerals
II	400−600	siderite, kerogen, pyrite, and structural water
III	>600	carbonate minerals (calcite, dolomite, and ankerite)

Table 1 shows that the shale sample has a relatively high ratio of carbonate minerals (calcite and dolomite) accounting for 53.5% of the total weight. For temperatures at 600−750 °C, carbonates rapidly decompose, and inter-layer water is released from clay minerals. This temperature range shows the largest weight loss from the TG-DTG curve (Figure 2). However, the weight changes at a temperature over 600 °C are complex because gas products from lower temperature regions might still react with the minerals and form different mineral phases. The work by Baruah and Tiwari illustrate macroscopic fractures and compositional changes occurring in oil/gas shales at high temperatures.[35] Equations 1−3 are the major reactions happening in the 600−800 °C region that can explain the reason for the weight loss for increasing temperature. Sulfur dioxide in eq 2 may be produced by pyrite oxidation. Bhargava et al. found that the reaction products could react again to produce new products, which are very difficult to measure.[21,24]

$$\text{calcite: } CaCO_3 \rightarrow CaO + CO_2(g) \quad (1)$$

$$CaCO_3 + SO_2 + \frac{1}{2}O_2(g) \rightarrow CaCO_4 + CO_2(g) \quad (2)$$

$$\text{dolomite: } [Ca, Mg]\,CO_3 \rightarrow [Ca, Mg]O + CO_2(g) \quad (3)$$

3.2. XRD Spectra. The XRD spectrum is quantitatively related to the weight ratio of each component in the rocks. Therefore, the weight ratio or concentration of each component can be obtained by comparing it with standard PDF cards of each mineral. The overall density is estimated by the summation of the product of the weight ratio and corresponding mineral density. Herein, shale samples processed under different temperatures were measured by an XRD analyzer to record the evolution of the geochemical composition. Figure 4a demonstrates the whole XRD patterns of the Wufeng−Longmaxi shale. The primary diffraction peaks can be indexed to the quartz, calcite, and dolomite phases. The

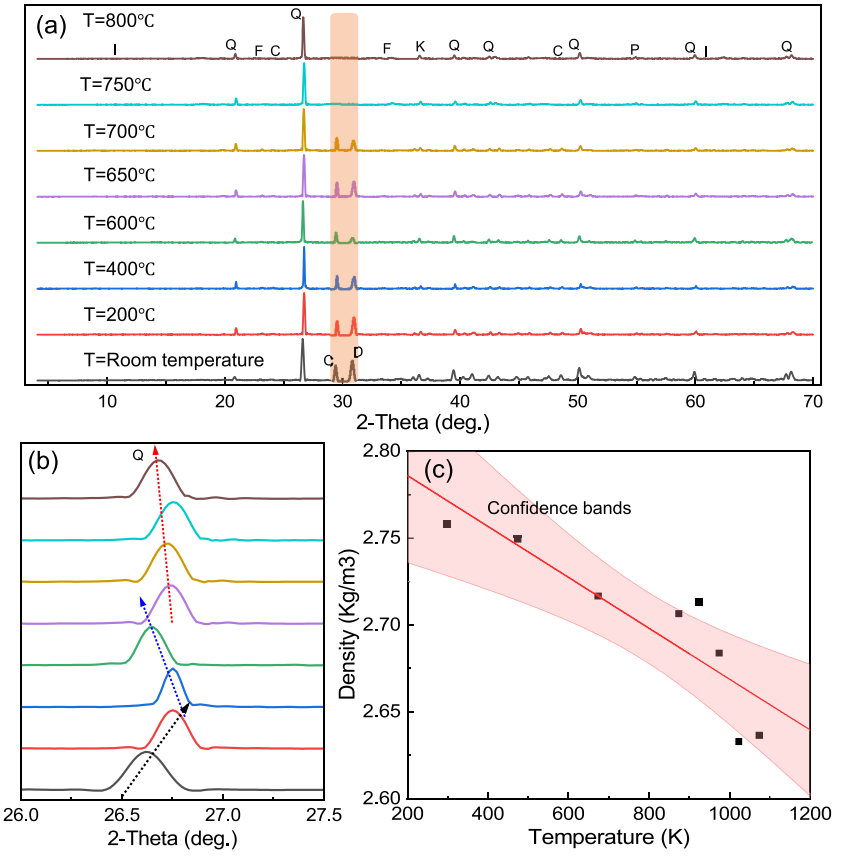

Figure 4. Quantitative analysis of XRD spectra and shale density evolution with the elevated temperature including (a) whole XRD patterns of shales at different temperatures, (b) enlarged XRD peaks at 26.6°, and (c) densities of shale with temperature. Notes: Q, quartz; F, feldspar; C, calcite; K, kaolinite; P, pyrite; I, illite; D, dolomite.

https://doi.org/10.1021/acsomega.2c03575
ACS Omega 2022, 7, 44689−44697

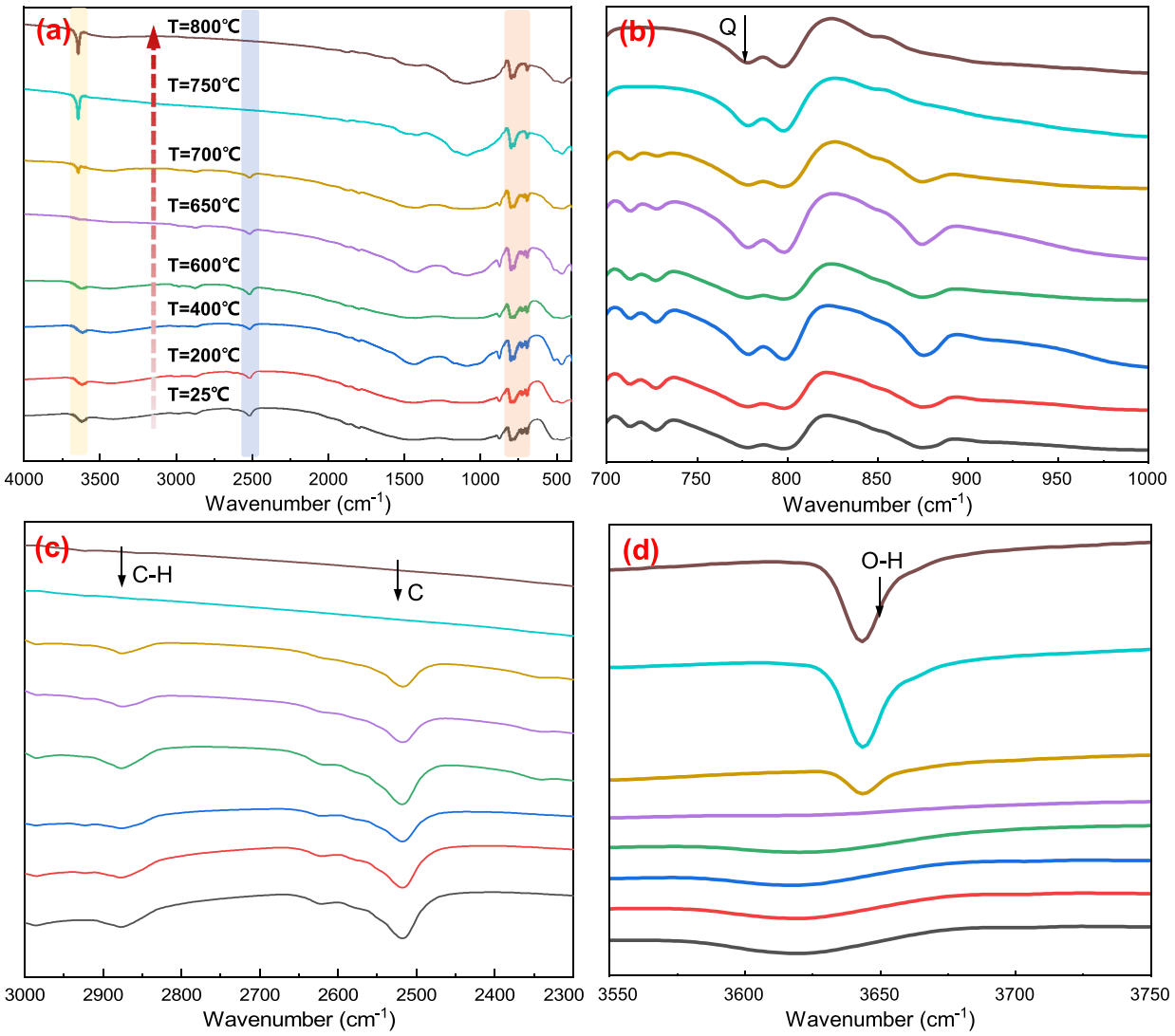

Figure 5. FTIR absorbance spectra of the Wufeng–Longmaxi shale under various temperatures. (a) FTIR absorption spectra under various temperatures; (b–d) characteristic absorption bands for quartz, carbonates, kerogen, and O–H bonds. Notes: Q, quartz; C, carbonate; C–H, organic matter; O–H, hydroxy group.

compositional information of shale samples varies with temperature. For instance, the diffraction peaks at 26.5° representing quartz have high stability with a small shift in the diffraction angle for the elevated temperature (Figure 4b). Diffraction peaks have a major change at the temperature between 600 and 800 °C, especially for calcite and dolomite. Variations of the indexed minerals (calcite and dolomite) due to chemical reactions can be derived from the XRD spectrum in Figure 4a.[28]Figure 4c shows that the densities of all shale samples linearly decrease with temperature caused by the big weight loss.

The intensity peak of carbonates (calcite, dolomite, etc.) is the second-highest located at the 2-theta of 29 and 31°. Illite is another important component, accounting for 94% of the clay content in Wufeng shale based on the clay analysis in Table 1. However, it cannot be detected through the analysis of the XRD spectra. It may be caused by the low concentration of the clay in the selected sample. According to the data from the existing research, similar results have been obtained because of the low intensity of clay contents.[36,37]

3.3. FTIR Spectra. Figure 5a illustrates the FTIR absorbance spectra of shale compositions under different temperatures. The wavenumber chosen for shale is in the mid-range spectra (400–4000 cm^{-1}) as presented. The FTIR results show the occurrence of the main compositions of quartz, kerogen, and carbonates. The quartz within shale has a high absorbance within the spectral range of 800–1000 cm^{-1}. Carbonates have a characteristic absorption band occurring between 1500 and 1400 cm^{-1} due to the internal vibrational modes of CO_3^{-2} ions. The spectrum peak of quartz emerges at 798–780 cm^{-1} due to the change of intermolecular bonds. Stretching vibrations of O–H emerge at 3750–3400 cm^{-1} to separate phyllosilicates from quartz. Kerogen's absorption spectrum exists between 1800 and 1000 cm^{-1} (C═O and C═C) and 3000 and 2800 cm^{-1}. These results show good agreement with the data of the work by Chen et al.[27]

Quartz has good thermal stability as its absorbance at around 800 cm^{-1} stays the same with the increase in temperature (Figure 5b). It can also be obtained from the XRD spectra presented in Figure 4a. Carbonates are stable at low temperatures but increasingly decompose at temperatures

https://doi.org/10.1021/acsomega.2c03575
ACS Omega 2022, 7, 44689–44697

Table 3. List of Experimental Parameters and Primary Results in the SHPB Tests

no. of samples	temperature (°C)	peakstrength (GPA)	strain rate (s^{-1})	maximum strain	dynamicYoung's modulus (GPA)	Tedesco−Ross DIF
T25-1	25	144.14	64.93	2.70	145.46	1.085
T25-2	25	133.07	80.43	3.49	133.12	1.155
T25-3	25	123.58	78.06	3.68	123.62	1.145
T200-1	200	149.30	72.04	3.30	149.30	1.119
T200-2	200	147.95	71.38	2.92	147.95	1.116
T200-3	200	147.47	60.66	2.64	147.64	1.062
T400-1	400	140.14	73.00	3.37	139.03	1.123
T400-2	400	127.47	63.86	3.21	128.07	1.079
T400-3	400	139.03	75.87	3.14	138.73	1.136
T500-1	500	120.63	90.09	4.01	120.63	1.193
T500-2	500	124.41	84.60	3.51	124.41	1.172
T500-3	500	130.94	85.35	3.19	130.94	1.175
T600-1	600	123.25	62.99	2.79	123.25	1.075
T600-2	600	147.21	72.78	3.08	147.21	1.112
T600-3	600	130.77	76.58	3.84	130.77	1.139
T700-1	700	129.48	80.50	3.36	129.48	1.156
T700-2	700	109.43	79.21	4.48	109.43	1.150
T700-3	700	108.26	81.66	4.10	108.26	1.160

over 400 °C. When the temperature exceeds 700 °C, the characteristic absorbance bands of calcite, carbonate, and C−H bands at 875, 2520, and 2875 cm^{-1}, respectively, completely disappear (Figure 5b,c). This reveals that a large proportion of carbonates of the Wufeng−Longmaxi shale have been decomposed at temperatures of 700 °C and above. The primary organic matter of kerogen in gas shale has been identified by the absorbance band at 2875 cm^{-1} in the FTIR spectra. The decomposition of organic matter usually starts at 400 °C and ends at about 750 °C according to the data in Figure 5c. Figure 5d shows a characteristic O−H absorption spectrum that emerges at temperatures of 700, 750, and 800 °C, which reveals new products occurring.

3.4. SHPB Test of Shale Samples at Different Temperatures. Table 3 provides the major parameters of peak strength, strain rate, maximum strain, and dynamic compressive strength in the SHPB tests. It shows that the peak strength of samples decreases for ascending temperature, which is identical to the evolution of dynamic compressive strength. Some typical stress−strain curves are presented in Figure 6 to demonstrate the correlation between temperature and the dynamic mechanical properties of shale. In the low-temperature region of 25−200 °C, little change occurs that is consistent with the result reported by Yang et al.[7] When the temperature is over 200 °C, the curves evolve rapidly with a decrease in the peak of stress. The slope of the post-peak curve decreases with the elevated temperature, indicating a reduction in rock brittleness.

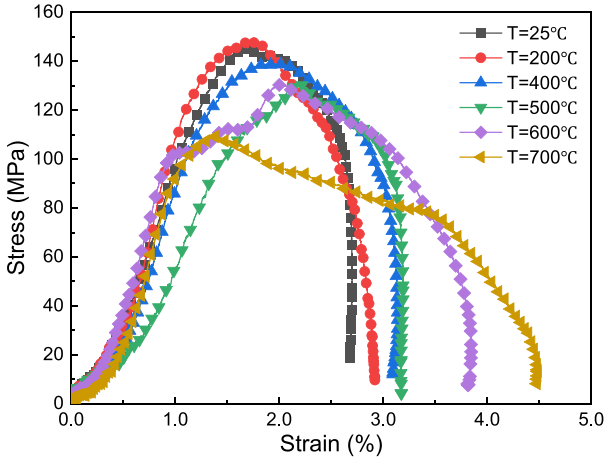

Figure 6. Dynamic stress−strain curves of shale samples at different temperatures from SHPB tests.

In the experimental process, we found the frequent occurrence of fractures in shale discs at a temperature between 300 and 400 °C. According to the work by previous researchers, water loss and partial organic decomposition can generate a significant increase in pore pressure.[14,21] When the temperature grows beyond 700 °C, all shale samples break into pieces. Therefore, all SHPB samples are prepared at the temperature range of 25−700 °C. Table 3 and Figure 7 present the mechanical parameters and the relationship of maximum strain and stress with temperature. The thermal stress inside rocks increases with temperature; meanwhile, the strength of shale is reduced with the elevated temperature. As a consequence, the shale samples break at a given high temperature.

4. DISCUSSION

Shale rock is a low-permeability sedimentary rock as well as a reservoir of oil and gas. As global interest in shale resources grows, theoretical and experimental works have been made for enhancing unconventional energy resources. Explosive fracturing techniques had been proposed in oil and gas production for decades and subsequently replaced by hydraulic fracturing.[5] Due to the enormous volume of water used in the hydraulic fracturing technique, researchers are looking for non-aqueous techniques, such as in situ explosive fracturing. Explosives applied in deep shale could generate complex fractures around drilling wells. In addition, the depleted shale reservoir has been also taken as a suitable place for nuclear waste disposal.[38−40] As a large amount of heat energy from the explosion and radioactive waste can cause a high reservoir temperature, the effects of high temperature on shale rocks should be investigated. The elevated temperature has been proven as a significant factor affecting the mechanical properties of rocks according to the published papers,[16,17,33,41] which could largely

https://doi.org/10.1021/acsomega.2c03575
ACS Omega 2022, 7, 44689−44697

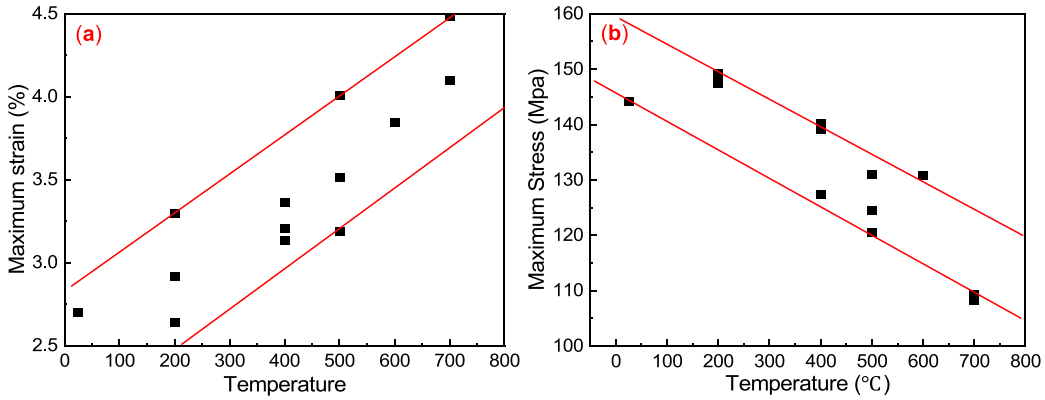

Figure 7. Measurements of mechanical strength and deformation of shale samples in SHPB tests including (a) maximum strain and (b) maximum stress evolution with temperature.

affect the performance of explosive fracturing and radioactive waste disposal. Therefore, a series of tests have been conducted in this work to quantitatively investigate the evolution of shale properties with temperature.

The TGA results in Figure 3 indicate a big weight loss of shale rocks with elevated temperatures. According to geochemistry, weight loss is caused by the physical/chemical reactions happening during the heating operation. The DTG curve shows that the reaction rate varies and reaches a peak at around 725 °C. It has been previously reported that the contained water is released from sedimentary rocks at below 200 °C, and chemical reactions of organic matter and minerals may begin at a temperature exceeding 300 °C.[21,24,42] XRD data in Figure 4a reveals that the thermal reaction of shale rocks contains several different reactions, such as pyrite oxidation, kerogen, and carbonate decomposition, by comparing with the XRD evolution curves of pure minerals. Figure 4b reveals a shift in the diffraction angle of the quartz peaks as a result of the increase in temperature. This transformation has been found in previous work and attributed to the rotation of the bonds between tetrahedral leads in the transition from α-quartz to β-quartz. Additionally, the evolution of carbonate minerals, including calcite and dolomite, has been directly observed through the XRD and FTIR absorbance spectra. It illustrates that there is a big weight loss in carbonate minerals of shale samples. This finding is consistent with the thermal properties of carbonates. However, it is unavoidable that gas products can react with other minerals and form new products.[35] Therefore, we can only tell the possible processes happening in a temperature range. It is challenging to provide the specific temperature and time of each mineral reaction.

The work by Longbottom et al. shows that the temperature-dependent phenomena are determined by the chemical reaction rate of shale contained minerals.[43] The temperature effect of the chemical reaction is commonly characterized by the Arrhenius relationship, which is expressed as

$$\frac{r}{r_0} = \exp\left[\frac{E_a}{R}\left(\frac{1}{T_0} - \frac{1}{T}\right)\right] \quad (4)$$

where r and r_0 represent the reaction rates (mol/s) at different temperatures of T and T_0 (K), respectively. E_a is the activation energy (KJ/mol), and R is the molar gas constant (KJ/mol/K). This expression gives the relationship between reaction rate and temperature. The reaction rates of minerals increase with T when activation energy E_a and the molar gas constant are known. It shows that the reaction inside shale varies when subjected to the increasing temperature. However, most minerals are very stable at room temperature and atmospheric pressure. The compositions of shale rocks are activated at various high temperatures. From the perspective of energy, when the input energy reaches the activation energy of a mineral, it can be activated and react with other matters.

The microscale reactions have dramatically altered the compositional information of shale samples. It is inevitable to have a great impact on the macroscopic mechanical properties. The temperature has been reported to have a significant impact on the hydro-mechanical properties of shale.[12,44] For temperatures below 400 °C, water evaporation can increase the pore pressure in the porous structure.[12] We found that some shale rocks burst apart in the muffle furnace at a temperature between 300 and 400 °C, which could be subjected to the increasing pore pressure exceeding the tensile strength. In our SHPB tests, there is a 25.6% reduction in dynamic Young's modulus of the shale rocks (Table 3) after the heating process in the muffle furnace. The dynamic stress−strain curves of six heated samples in Figure 6 provide a reduction of rock brittleness. This reveals the brittle to ductile transition in shale rocks due to the heated decomposition of the brittle minerals.[45] In this process, the strength of the shale sample linearly decreases while the maximum strain linearly increases with temperature (Figure 7a,b). High temperatures providing high thermal stress can cause damage to rocks according to the theory of thermodynamics.[46−48] Our tests found that shale samples rapidly explode into pieces at 800 °C.

5. CONCLUSIONS

This paper presents an investigation of the effect of temperature on the compositional and mechanical properties of the Wufeng−Longmaxi shale. Results indicate that temperature has a great influence on both the composition and dynamic mechanical properties of shale rocks. An integrated method with TGA, XRD, and FTIR is introduced to characterize the compositional information of shale samples evolving with the elevated temperature. The SHPB is applied to test the changes in the dynamic mechanical properties. Conclusions have been made as follows.

(1) There is a 25% weight loss in shale powders measured with TGA at a heating rate of 10 °C/min. A little reduction in the sample's weight occurs before 400 °C, but a big weight loss emerges at a temperature of 600−750 °C due to mineral reactions. According to the TG-DTG curve, the evolution of

https://doi.org/10.1021/acsomega.2c03575
ACS Omega 2022, 7, 44689−44697

the shale weight with temperature is divided into three stages concerning the thermal decomposition of different compositions of the Wufeng−Longmaxi shale.

(2) The XRD-FTIR combined method identifies the effect of temperature on the compositional information of shale rocks. XRD and FTIR spectra both illustrate that the decomposition of kerogen and carbonate minerals primarily governs the weight and density decreases observed from TGA data. It is also found that a change in the X-ray incidence angle of quartz is due to the transition from α-quartz to β-quartz. FTIR spectra reveal reactions to produce new products with O−H absorbance bands happening for temperatures above 700 °C.

(3) This provides a direct relationship between compositional information and macroscopic mechanical properties through the SHPB tests. The evolution of the shale composition with temperature has a great impact on the dynamic strength. A brittle to ductile transition has occurred due to the changes in the compositional information.

AUTHOR INFORMATION

Corresponding Author

Cheng Zhai − *Key Laboratory of Coal Methane and Fire Control, Ministry of Education and School of Safety Engineering, China University of Mining and Technology, Xuzhou, Jiangsu 221116, China;* orcid.org/0000-0001-9256-1494; Email: greatzc@cumt.edu.cn

Authors

Xu Yu − *Key Laboratory of Coal Methane and Fire Control, Ministry of Education, Jiangsu Key Laboratory of Coal-Based Greenhouse Gas Control and Utilization, and School of Safety Engineering, China University of Mining and Technology, Xuzhou, Jiangsu 221116, China;* orcid.org/0000-0002-5354-6723

Yu Jing − *School of Minerals and Energy Resources Engineering, UNSW, Sydney 1001, Australia*

Shuxun Sang − *Jiangsu Key Laboratory of Coal-Based Greenhouse Gas Control and Utilization and Key Laboratory of Coalbed Methane Resources and Reservoir Formation Process, Ministry of Education, China University of Mining and Technology, Xuzhou, Jiangsu 221116, China;* orcid.org/0000-0001-6246-6728

Yu Wang − *Key Laboratory of Coal Methane and Fire Control, Ministry of Education and School of Safety Engineering, China University of Mining and Technology, Xuzhou, Jiangsu 221116, China*

Klaus Regenauer-Lieb − *School of Mines: Minerals, Energy and Chemical Engineering, Curtin University, Perth 6000, Australia*

Yong Sun − *Key Laboratory of Coal Methane and Fire Control, Ministry of Education and School of Safety Engineering, China University of Mining and Technology, Xuzhou, Jiangsu 221116, China;* orcid.org/0000-0001-8327-7870

Complete contact information is available at: https://pubs.acs.org/10.1021/acsomega.2c03575

Author Contributions

X.Y.: conceptualization, data curation, methodology, and writing; C.Z.: supervision and project administration; Y.J.: writing-reviewing and editing; S.S. and K.R.-L.: writing-reviewing and editing and supervision; Y.W.: investigation and visualization; Y.S.: data curation.

Notes

The authors declare no competing financial interest.

ACKNOWLEDGMENTS

This work was financially supported by the National Key R&D Program of China (2020YFA0711800), the National Natural Science Foundation of China (51774278 and 52104233), the Jiangsu High-Level Personnel Project (JSSCBS20211235), and the Fundamental Research Funds for the Central Universities (2021QN1091).

REFERENCES

(1) Zoback, M. D. A. K.; Arjun, H.*Unconventional reservoir geomechanics: Shale Gas, Tight Oil, and Induced Seismicity*; Cambridge University Press: 2019, DOI: 10.1017/9781316091869.

(2) Rezaee, R.*Fundamentals of Gas Shale Reservoirs*; John Wiley & Sons: 2015.

(3) Wang, Q.; Li, R. Research status of shale gas: A review. *J. Renewable Sustainable Energy Rev.* **2017**, *74*, 715−720.

(4) Lee, K. S. A. K.; Tae, Hong. *Integrative Understanding of Shale Gas Reservoirs*; Springer: 2016, DOI: 10.1007/978-3-319-29296-0.

(5) Grady, D. E.; Kipp, M. E. Continuum modelling of explosive fracture in oil shale. *Int. J. Rock Mech. Mining Sci. Geomech. Abstr.* **1980**, *17*, 147−157.

(6) Suo, Y.; Chen, Z.; Rahman, S. S. Changes in Shale Rock Properties and Wave Velocity Anisotropy Induced by Increasing Temperature. *Nat. Resour. Res.* **2020**, *29*, 4073−4083.

(7) Yang, G.; Liu, J.; Li, X.; Bi, J. Effect of temperature on shale strength under dynamic impact loading. *Arabian J. Geosci.* **2020**, *13*, 1.

(8) Rexer, T. F. T.; Benham, M. J.; Aplin, A. C.; Thomas, K. M. Methane Adsorption on Shale under Simulated Geological Temperature and Pressure Conditions. *Energy Fuels* **2013**, *27*, 3099.

(9) Zou, J.; Rezaee, R.; Liu, K. Effect of Temperature on Methane Adsorption in Shale Gas Reservoirs. *Energy Fuels* **2017**, *31*, 12081−12092.

(10) De Bruyn, D.; Thimus, J.-F. The influence of temperature on mechanical characteristics of Boom clay: the results of an initial laboratory programme. *J. Eng. Geol.* **1996**, *41*, 117−126.

(11) Masri, M.; Sibai, M.; Shao, J.-F.; Mainguy, M. Experimental investigation of the effect of temperature on the mechanical behavior of Tournemire shale. *Int. J. Rock Mech. Mining Sci.* **2014**, *70*, 185−191.

(12) Braun, P.; Ghabezloo, S.; Delage, P.; Sulem, J.; Conil, N. Thermo-Poro-Elastic Behaviour of a Transversely Isotropic Shale: Thermal Expansion and Pressurization. *Rock Mech. Rock Eng.* **2021**, *54*, 359−375.

(13) Zhou, H.; Liu, H.; Hu, D.; Yang, F.; Lu, J.; Zhang, F. Anisotropies in Mechanical Behaviour, Thermal Expansion and P-Wave Velocity of Sandstone with Bedding Planes. *Rock Mech. Rock Eng.* **2016**, *49*, 4497−4504.

(14) Torrente, M. C.; Galán, M. A. Kinetics of the thermal decomposition of oil shale from Puertollano (Spain). *Fuel* **2001**, *80*, 327−334.

(15) Cekerevac, C.; Laloui, L. Experimental study of thermal effects on the mechanical behaviour of a clay. *Int. J. Numer. Anal. Methods Geomech.* **2004**, *28*, 209−228.

(16) Feng, Z.-j.; Qiao, M.-m.; Dong, F.-k.; Yang, D.; Zhao, P. Thermal Expansion of Triaxially Stressed Mudstone at Elevated Temperatures up to 400 degrees C. *Adv. Mater. Sci. Eng.* **2020**, *2020*, 8140739.

(17) Kumar, V.; Sondergeld, C.; Rai, C. S. Effect of mineralogy and organic matter on mechanical properties of shale. *Interpretation* **2015**, *3*, SV9−SV15. Interpretation (acccessed 4/27/2022)

(18) Liu, X.; Zhang, C.; Yuan, S.; Fityus, S.; Sloan, S. W.; Buzzi, O. Effect of High Temperature on Mineralogy, Microstructure, Shear

Stiffness and Tensile Strength of Two Australian Mudstones. *Rock Mech. Rock Eng.* **2016**, *49*, 3513−3524.
(19) Zhang, C.; Dong, D.; Wang, Y.; Guan, Q. Brittleness evaluation of the Upper Ordovician Wufeng-Lower Silurian Longmaxi shale in Southern Sichuan Basin, China. *Energy Explor. Exploit.* **2017**, *35*, 430−443.
(20) Kang, Y.; Shang, C.; Zhou, H.; Huang, Y.; Zhao, Q.; Deng, Z.; Wang, H.; Ma, Y. Z. Mineralogical brittleness index as a function of weighting brittle minerals-from laboratory tests to case study. *J. Nat. Gas Sci. Eng.* **2020**, *77*, No. 103278.
(21) Bhargava, S.; Awaja, F.; Subasinghe, N. D. Characterisation of some Australian oil shale using thermal, X-ray and IR techniques. *Fuel* **2005**, *84*, 707−715.
(22) You, J.; Lee, K. J. The experimental investigation and data−driven modeling for thermal decomposition kinetics of Green River Shale. *Fuel* **2022**, *320*, No. 123899.
(23) Senthil Kumar, R.; Rajkumar, P. Characterization of minerals in air dust particles in the state of Tamilnadu, India through FTIR, XRD and SEM analyses. *Infrared Phys. Technol.* **2014**, *67*, 30−41.
(24) Fan, C.; Yan, J.; Huang, Y.; Han, X.; Jiang, X. XRD and TG-FTIR study of the effect of mineral matrix on the pyrolysis and combustion of organic matter in shale char. *Fuel* **2015**, *139*, 502−510.
(25) Torrente, M. C.; Galán, M. A. Kinetics of the thermal decomposition of oil shale from Puertollano (Spain). *Fuel* **2001**, *80*, 327−334.
(26) Xu, Z.; Bahne, C. C.; Domenic, C. P.; Wayne, D. P.; James, R. W.; Hwang, J. Quantitative Mineral Analysis by FTIR Spectroscopy. *Internet J. Vib. Spectrosc.* **2001**, *5*, 12.
(27) Chen, Y.; Furmann, A.; Mastalerz, M.; Schimmelmann, A. Quantitative analysis of shales by KBr-FTIR and micro-FTIR. *Fuel* **2014**, *116*, 538−549.
(28) Kumar, R. S.; Rajkumar, P. Characterization of minerals in air dust particles in the state of Tamilnadu, India through FTIR, XRD and SEM analyses. *Infrared Phys. Technol.* **2014**, *67*, 30−41.
(29) Liang, C.; Jiang, Z.; Yang, Y.; Wei, X. Shale lithofacies and reservoir space of the Wufeng−Longmaxi Formation, Sichuan Basin, *China. Pet. Explor. Dev.* **2012**, *39*, 736−743.
(30) Tang, X.; Jiang, S.; Jiang, Z.; Li, Z.; He, Z.; Long, S.; Zhu, D. Heterogeneity of Paleozoic Wufeng-Longmaxi formation shale and its effects on the shale gas accumulation in the Upper Yangtze Region, China. *Fuel* **2019**, *239*, 387−402.
(31) Zhang, W.; Hu, W.; Borjigin, T.; Zhu, F. Pore Characteristics of Different Organic Matter in Black Shale: A Case Study of the Wufeng-Longmaxi Formation in the Southeast Sichuan Basin, China. *Mar. Pet. Geol.* **2020**, *111*, 33.
(32) Xu, H.; Zhou, W.; Zhang, R.; Liu, S.; Zhou, Q. Characterizations of pore, mineral and petrographic properties of marine shale using multiple techniques and their implications on gas storage capability for Sichuan Longmaxi gas shale field in China. *Fuel* **2019**, *241*, 360−371.
(33) Murrell, S. A. F.; Ismail, I. A. H. The effect of decomposition of hydrous minerals on the mechanical properties of rocks at high pressures and temperatures. *Tectonophysics* **1976**, *31*, 207−258.
(34) Galan, M.; Smith, J. Pyrolysis of oil shale: experimental study of transport effects. *AIChE J.* **1983**, *29*, 604−610.
(35) Baruah, B.; Tiwari, P. J. A. J. Compositional and kinetic study of thermal degradation of kerogen using TG-FTIR, NMR, and microscopic study. *AIChE J.* **2022**, *68*, No. e17396.
(36) Repacholi, M.*Clay mineralogy: spectroscopic and chemical determinative methods*; Springer Science & Business Media: 2012.
(37) Haldar, S. K.*Introduction to mineralogy and petrology*; Elsevier: 2020, DOI: 10.1016/B978-0-12-820585-3.00004-1.
(38) Chapman, N. A.; McKinley, I. G.; Hill, M. D.*The geological disposal of nuclear waste*; John Wiley and Sons: 1987.
(39) Chang, K. W.; Nole, M.; Stein, E. R. Reduced-order modeling of near-field THMC coupled processes for nuclear waste repositories in shale. *Comput. Geotech.* **2021**, *138*, No. 104326.
(40) Neuzil, C. Can shale safely host US nuclear waste? *Eos, Trans. Am. Geophys. Union* **2013**, *94*, 261−262.
(41) Hachemi, S.; Rahmouni, Z. E. A Review on the Effect of Varied Sand Types in Concrete at High Temperature. *J. Eng. Res. Sci.* **2022**, *1*, 38−47.
(42) Zhang, H.; Huang, H.; Li, Z.; Liu, M.; Jiang, C.; Xu, X. Thermal stability and parameter validity of hopane series in mature shales − A case study from Dongying Depression, eastern China. *Fuel* **2022**, *315*, No. 123222.
(43) Longbottom, T. L.; Hockaday, W. C.; Daigle, H.; Harvey, O. R.*Organic chemical structure relationships to maturity and stability in shales. Int. J. Coal Geol.*2020, *223*, 103448, DOI: 10.1016/j.coal.2020.103448.
(44) Liu, J.; Xue, Y.; Zhang, Q.; Yao, K.; Liang, X.; Wang, S. Micro-cracking behavior of shale matrix during thermal recovery: Insights from phase-field modeling. *Eng. Fract. Mech.* **2020**, *239*, No. 107301.
(45) Gutierrez, M.Effects of stress, anisotropy and brittle-to-ductile transition on fracturing and fluid flow in shales. In *ISRM European Rock Mechanics Symposium-EUROCK 2018*; OnePetro: 2018.
(46) Gautam, P. K.; Dwivedi, R.; Kumar, A.; Kumar, A.; Verma, A. K.; Singh, K. H.; Singh, T. N. Damage Characteristics of Jalore Granitic Rocks After Thermal Cycling Effect for Nuclear Waste Repository. *Rock Mech. Rock Eng.* **2021**, *54*, 235−254.
(47) Castagna, A.; Ougier-Simonin, A.; Benson, P.; Browning, J.; Walker, R. J.; Fazio, M.; Vinciguerra, S. Thermal damage and pore pressure effects of the Brittle-Ductile transition in comiso limestone. *J. Geophys. Res.: Solid Earth* **2018**, *123*, 7644−7660.
(48) Liu, L.; Ji, H.; Elsworth, D.; Zhi, S.; Lv, X.; Wang, T. Dual-damage constitutive model to define thermal damage in rock. *Int. J. Rock Mech. Mining Sci.* **2020**, *126*, No. 104185.

https://doi.org/10.1021/acsomega.2c03575
ACS Omega 2022, 7, 44689−44697